Numerical modelling of thermal phenomenon in friction stir welding of aluminum plates

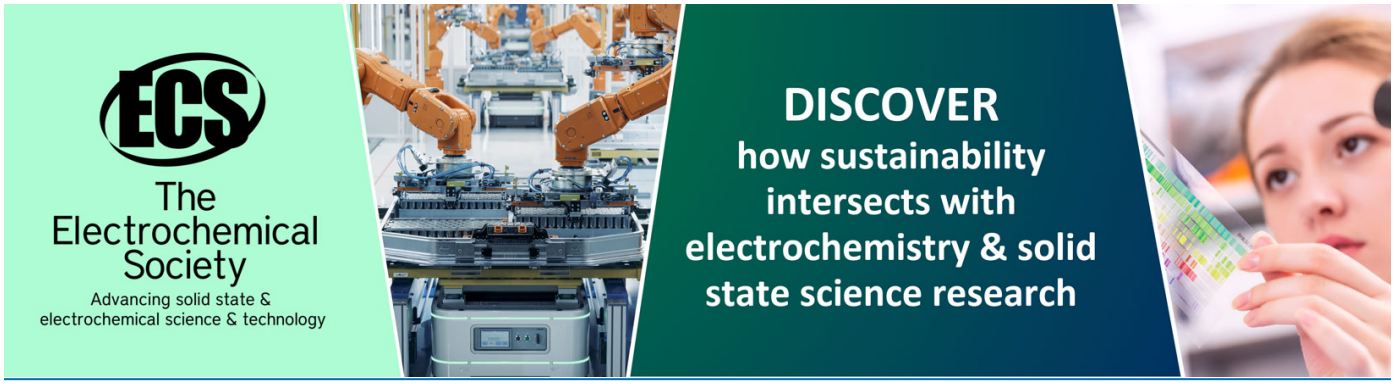

Numerical modelling of thermal phenomenon in friction stir welding of aluminum plates

R Vaira Vignesh, R Padmanaban*, M Arivarasu, S Thirumalini,J Gokulachandran and Mutyala Sesha Satya Sai Ram

Department of Mechanical Engineering, Amrita School of Engineering, Coimbatore, Amrita Vishwa Vidyapeetham, Amrita University, India

dr_padmanaban@cb.amrita.edu

Abstract. Friction stir welding (FSW) is a solid state welding process with potential to join materials that are non weldable by conventional fusion welding techniques. The study of heat transfer in FSW aids in the identification of defects like flash, inadequate heat input, poor material flow and mixing etc. In this paper, transient temperature distribution during FSW of aluminum alloy AA6061-T6 was simulated using finite element modelling. The model was used to predict the peak temperature and analyse the thermal history during FSW. The effect of process parameters namely tool rotation speed, tool traverse speed (welding speed), shoulder diameter and pin diameter of tool on the temperature distribution was investigated using two level factorial design. The model results were validated using the experimental results from the published literature. It was found that peak temperature was directly proportional to tool rotation speed and shoulder diameter and inversely proportional to tool traverse speed. The effect of pin diameter on peak temperature was found to be trivial.

1. Introduction

The necessity in automotive industry for light weighting, demands for selection and joining of lightweight materials with precision [1-3]. Aluminum is the primary choice in the drive for lean weight vehicles. Conventional fusion welding process fail to produce sound welds in aluminum alloys due to the formation of aluminum oxide layer. Friction Stir Welding is a solid state welding technique in which material is joined by the heat generated due to the combined effect of rotation and sliding motion of the tool under an axial load. The schematic of FSW is given in Figure 1. The heat generation due to friction and plastic flow results in defect free high quality welds in ferrous and non-ferrous materials [4]. FSW can be used to join most of the aluminum alloys which are difficult to weld by conventional fusion processes. The potential scope for FSW lies with joining non-ferrous materials ranging from aluminum, copper, lead, titanium, zinc and alloys etc.

In FSW process, a specially shaped rotating tool is made to traverse through the abutting faces of the joint. The relative motion between the tool and the substrate generates frictional heat. The translation of the rotating tool along the joint line (i.e. forward) under axial load causes plasticised material flow resulting in solid phase joint behind the tool [5-7]. If the tool is modelled as traversing

heat source, the traverse of tool would necessitate a complex model. In this paper, a moving coordinate system fixed at the tool axis was used for the analysis. The heat transfer of the plates become a stationary heat convection – heat conduction problem after the transformation of coordinate system. In this model, the plates were assumed to be infinite in length. The heat transfer analysis is neglected near the edge boundaries of the plate [8]. In this paper, the effect of tool rotation speed (TRS), tool traverse speed (TTS), shoulder diameter (SD) and pin diameter (PD) on temperature distribution was investigated using factorial design.

Nomenclature

Sl.	Name	Description	Units
1	T_o	Ambient temperature	K
2	T_{melt}	Melting temperature of work piece	K
3	h_u	Heat transfer coefficient on upside of work piece	W / m^2K
4	h_d	Heat transfer coefficient on downside of work piece	W / m^2K
5	Є	Surface emissivity	-
6	U	Welding speed or Tool traverse speed	m / s
7	μ	Coefficient of friction	-
8	N	Tool rotation speed	Rpm
9	ω	Angular velocity	rad / s
10	F_n	Plunge force	N
11	r_{pin}	Radius of pin	Mm
12	$r_{shoulder}$	Radius of shoulder	Mm
13	q_{pin}	Pin heat source	W
14	$q_{shoulder}$	Shoulder heat source	W
15	q_u	Heat flux on upper side of work piece	W / m^2
16	q_d	Heat flux on lower side of work piece	W / m^2
17	A_s	Surface area of shoulder	m^2
18	ρ	Density	kg / m^3

2. Finite Element Modelling

The FSW model used in this study generated using Comsol Multi physics 5.0 software. The model geometry is shown in Figure 2. The dimensions of the model were 400 mm × 200 mm × 3 mm surrounded by two infinite domains along x - axis. The model developed is as shown in the Figure 2. Non uniform boundary conditions were defined as the temperature at the upper side of the work piece changes with respect to time and variation in process parameters [8].

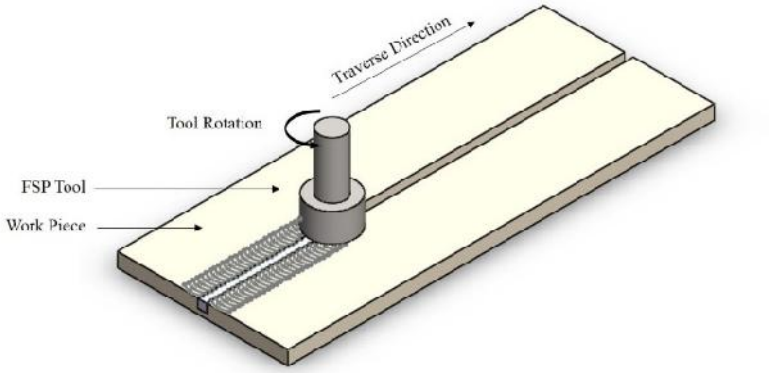

Figure 1 Schematic of FSW of aluminum plates

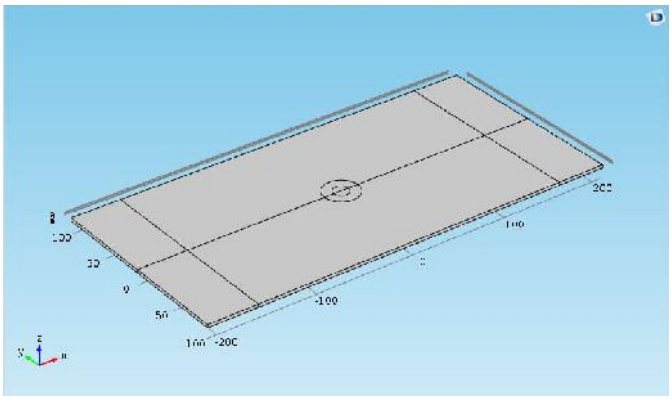

Figure 2 Model geometry of FSW

2.1. Heat transfer

The convective boundary condition specifies the heat transfer between the upper side of the work piece and the environment. As convective heat losses occur in all the free surfaces, convection co-efficient of h_u and h_d was applied to the upside and downside surfaces of the work piece. The contact conductance between the downside of the work piece and backing plate was modelled by an enhanced heat transfer coefficient. The surface boundary condition at the interface of the tool - workpiece was calculated from the frictional heat.

The heat transfer in the plate is governed by the following equation (1).

$$\rho C_p u . \nabla T + \nabla . (-k \nabla T) = Q \quad (1)$$

The upper side and down side of the plate loss heat due to natural convection and due to surface to ambient condition radiation. The corresponding heat fluxes at the upper and lower surface are given by the following equation (2)and equation (3).

$$q_u = h_u (T_0 - T) + \epsilon \sigma (T_{amb}^4 - T^4) \quad (2)$$

$$q_d = h_d (T_0 - T) + \epsilon \sigma (T_{amb}^4 - T^4) \quad (3)$$

2.2. Heat generation

The heat generated at the interface between the tool's pin and the plate as surface heat source is given by the followingequation (4).

$$q_{pin}(T) = \frac{\mu}{\sqrt{3(1+\mu)^2}} r_p \omega Y(T) \quad (4)$$

Where Y(T) is the average shear stress as a function of temperature. This function has been interpolated from the experimental results.

The heat generated at the interface between the tool's shoulder and the plate as surface heat source is given by the followingequation (5).

$$q_{shoulder}(r,T) = \begin{cases} \mu (F_n / A_s) \omega r, & \text{if } T < T_{melt} \\ 0, & \text{if } T > T_{melt} \end{cases} \quad (5)$$

2.3. Material property

The coefficient of friction was taken as 0.27. The temperature dependent yield stress of the material was correlated with the viscosity of the material as given in Figure 3. The temperature dependent properties in the present work can be found in the literature elsewhere [9-16]. The plot of Yield stress vs Temperature was obtained from the experimental work [17].

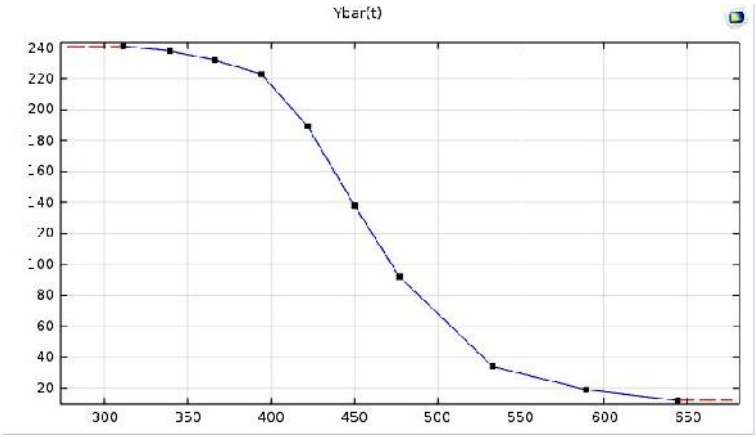

Figure 3 Yield stress vs Temperature for AA6061-T6 [17]

3. Model validation

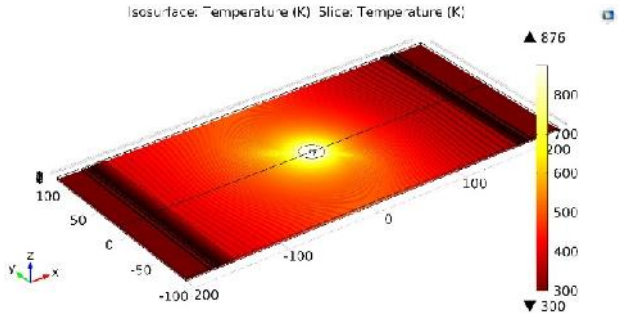

Figure 4 Iso surface temperature plot

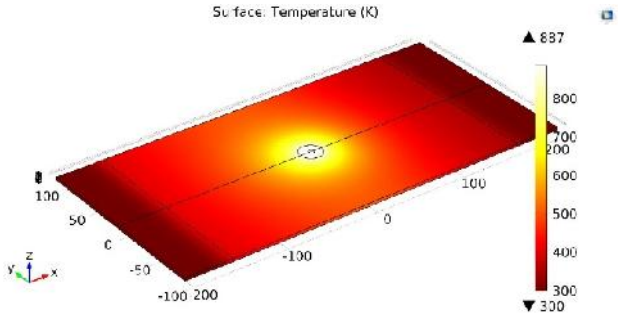

Figure 5 Surface temperature plot

The model was first applied to simulate the experimental work on FSW of AA 6061-T6 carried out by Hwang et al [18]. The experimental temperature measurements was made using four thermo couple units placed equally at a distance of 5 mm, along the traverse direction of the tool. The TRS, TTS, SD and PD was 920 rpm, 0.33 mm/s, 12 mm and 3 mm respectively. The temperature profile of the

friction stir welded AA6061-T6 plates using the developed model is as shown in the Figure 4 and Figure 5 .

In the model, the temperature of the plate was measured using 10 probes equally spaced at a distance of 5 mm from the pin of the tool.The computed temperature of the plate at different probes are as given in Table 1.

Table 1 Computed temperature of the validation model (in Kelvin)

TRS	TTS	SD	PD	Probe 1	Probe 2	Probe 3	Probe 4	Probe 5	Probe 6	Probe 7	Probe 8	Probe 9
920	0.33	12	3	463.38	503.35	556.62	624.24	663.20	597.28	513.31	452.91	411.14

The comparison of predicted temperature with experimental values is depicted Figure 6. As noted in the Figure 6, a very close agreement is observed between the computed and experimental temperatures. The minor difference in temperature between the experimental and computed value at is attributed to the assumed convective boundary condition for the backing plate in the generated model [19]. Thus the temperature prediction efficacy of the generated model was validated.

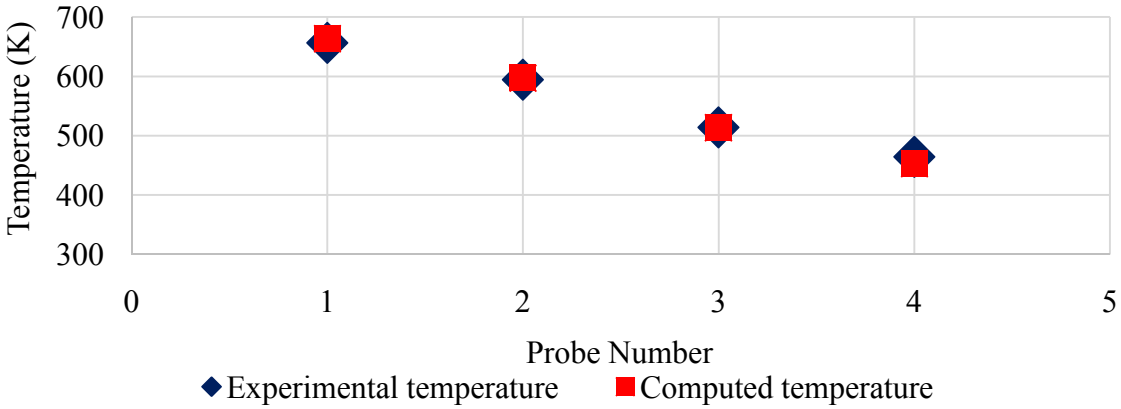

Figure 6 Temperature vs Displacement for FSW AA6061-T6 (Experimental and Computed)

4. Experimental design

It is evident from the equations equation (1), equation (4) and equation (5) that the TRS, TTS, SD and PD process parameters play a vital role in the heat transfer during FSW. The main and combined effect of these parameters upon the peak temperature (T_p) near the pin was analysed using 2^k factorial design.

Table 2 Coded and Real value

Coded Value	Real Value of process parameters			
	TRS (rpm)	TTS (mm / s)	SD (mm)	PD (mm)
-1	900	0.50	15	5
1	1200	1.00	21	7

The parameters and their levels are shown in Table 2. Four parameters with two levels was chosen for conducting experiments in this study. The experimental design matrix has sixteen factorial runs.

5. Results and Discussion

The T_p obtained during FSW of aluminum plates with various process parameters is as given in Table 3Table 3. It is observed that the T_p obtained is independent of variation in PD.

Table 3 Computed peak temperature during FSW

Sl.	Real value of process parameters				Computed T_p (K)
	TRS (rpm)	TTS (mm/s)	SD (mm)	PD (mm)	
1	900	0.5	15	5	696.96
2	900	0.5	15	7	697.07
3	900	0.5	21	5	765.88
4	900	0.5	21	7	765.90
5	900	1	15	5	683.49
6	900	1	15	7	683.59
7	900	1	21	5	756.50
8	900	1	21	7	756.56
9	1200	0.5	15	5	697.14
10	1200	0.5	15	7	697.23
11	1200	0.5	21	5	766.06
12	1200	0.5	21	7	766.11
13	1200	1	15	5	683.68
14	1200	1	15	7	683.76
15	1200	1	21	5	756.72
16	1200	1	21	7	756.95

As the variation of PD (5 mm and 7 mm) has insignificant effect on the temperature distribution, the plots obtained were similar. Hence the surface plot of the temperature profile (for both PD) is as given in Figure 7. The Pareto chart of the effects of process parameters on obtaining the peak temperature is given in Figure 8. It is observed that the SD is very imperative in obtaining the peak temperature. Evidently the TTS also plays vital role in obtaining the T_p. The TRS also contributes to obtain T_p as the heat generation in pin is proportional to the angular velocity of the tool.

The main effects of the process parameters in obtaining the T_p during FSW is shown in Figure 9. The heat generation at the pin is proportional to the TRS. But the effect of TRS in heat generation is lower than that of the other parameters and their combined effect. The amount of heat produced is dependent on the contact area of tool with that of the work piece. Hence the increase of SD essentially increased the T_p obtained during FSW. The TTS affects the generation of heat at the interface and transfer of heat to the plates from the tool's pin. The amount of heat transferred and frictional heat generated is proportional to the contact time of tool – workpiece interface. The increase in TTS results in decreased contact time. So there is reduction in T_p with increase in TTS.

SD = 15 mm

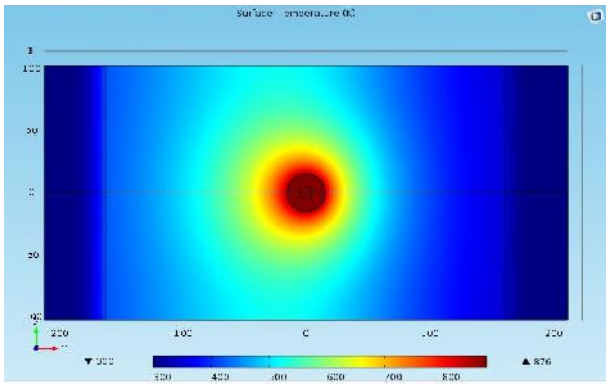

(a) TRS = 900 rpm; TTS = 0.5 mm/s

SD = 21 mm

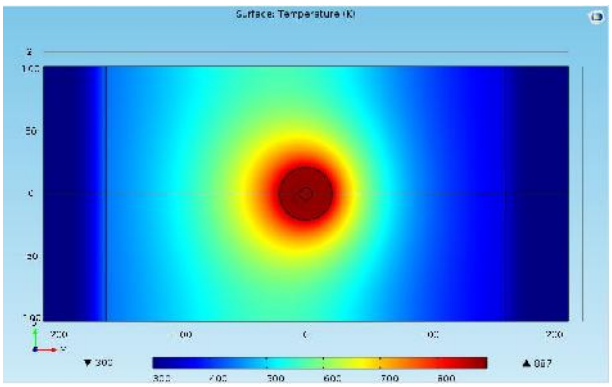

(b) TRS = 900 rpm; TTS = 0.5 mm/s

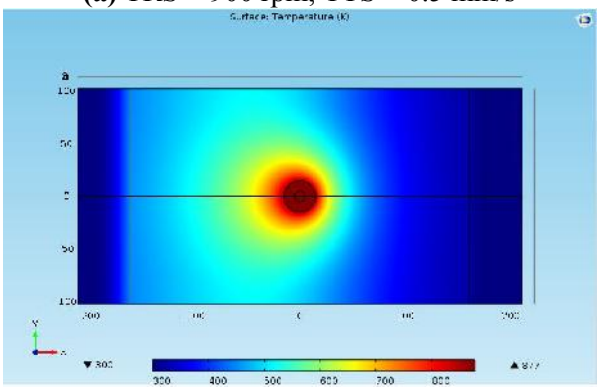

(c) TRS = 900 rpm; TTS = 1.0 mm/s

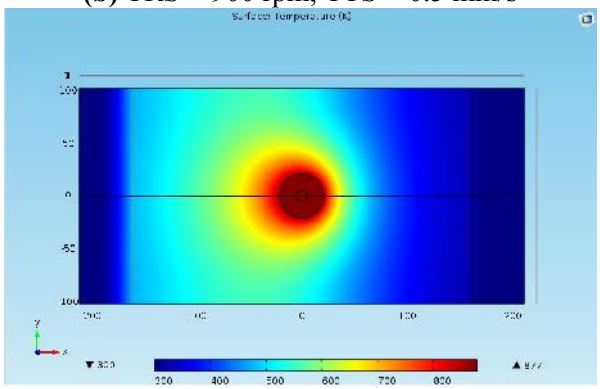

(d) TRS = 900 rpm; TTS = 1.0 mm/s

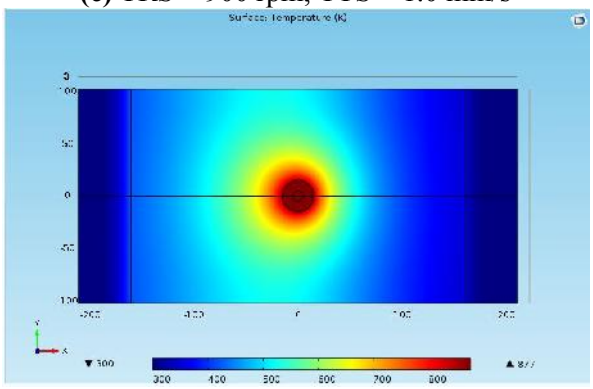

(e) TRS = 1200 rpm; TTS = 0.5 mm/s

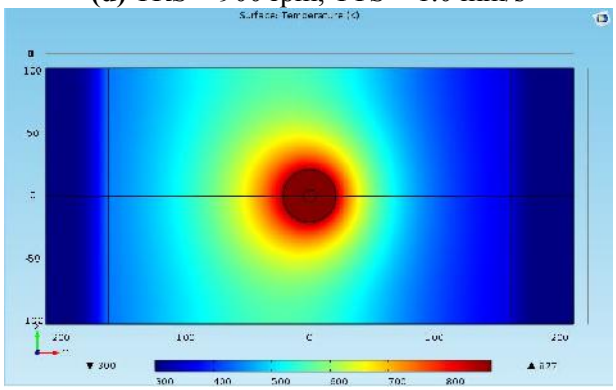

(f) TRS = 1200 rpm; TTS = 0.5 mm/s

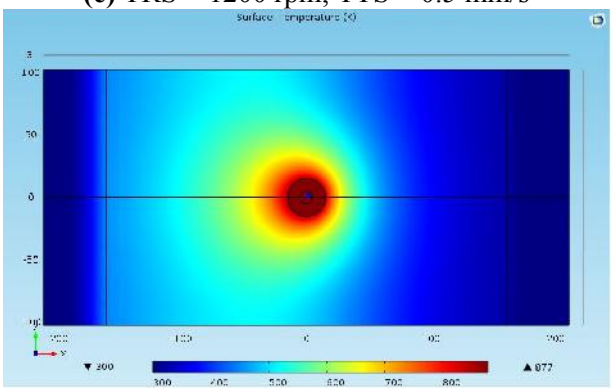

(g) TRS = 1200 rpm; TTS = 1.0 mm/s

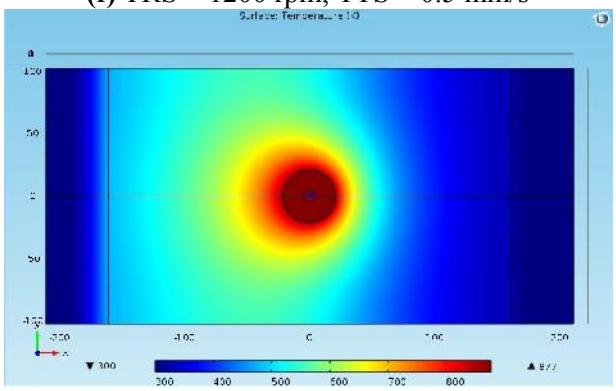

(h) TRS = 1200 rpm; TTS = 1.0 mm/s

Figure 7 Surface Temperature plot of FSW with various process paramters @ PD = 5 mm and 7 mm

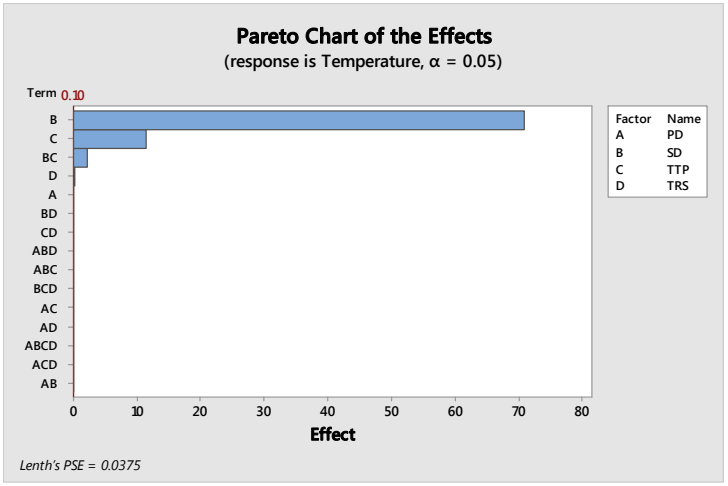

Figure 8 Pareto chart of the process parameters

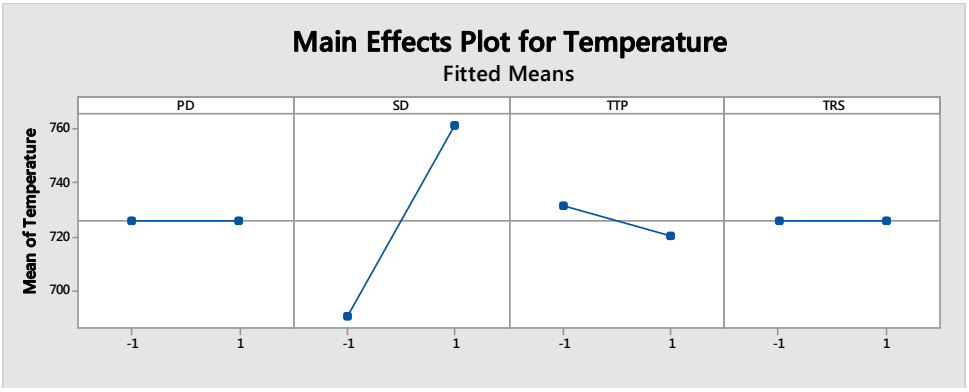

Figure 9Main effects of process parameters

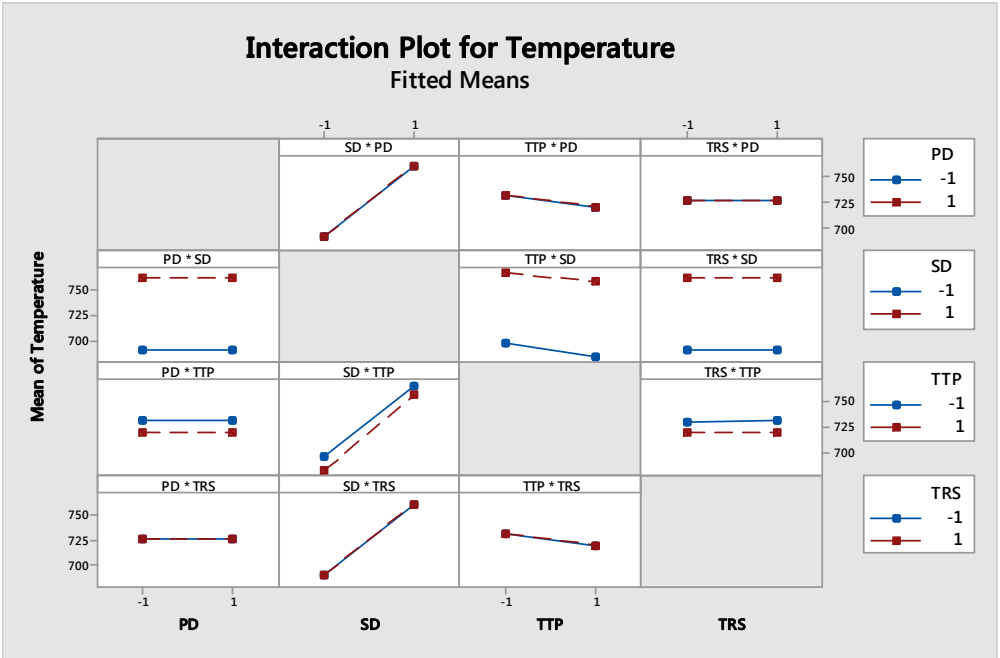

Figure 10 Interaction effects of parameters

The interaction effect of the process parameters in obtaining the T_p is as shown inFigure 9. The combined effects of the process parameters are same irrespective of the variation in process level. As discussed earlier, the interaction of PD*TRS is less significant.The increase in SD (SD*TRS) increased the $T_p$and increase in TTP (TTP*TRS) decreased the T_p. The combined effect of PD*TTP, SD*TTP and TRS*TTP is such that at high level of TTS, there is significant decrease in the T_p. The interaction of PD*TTP and TRS*TTP is less significant. The increase in SD (SD*TTP) decreased T_p irrespective of TTP. The increased surface area resulted in heat generation at the interface of tool – workpiece. But the heat transfer rate from tool to the workpiece is reduced at high TTS resulting in reduced T_p. The combined effect of PD*SD, TTP*SD and TRS*SD is such that increase in SD increased the T_p. The increase in SD of PD*SD and TRS*SD increased the T_p.The combined effect of SD*PD, TTP*PD and TRS*PD is same irrespective of the variation. The increase in SD (SD*PD) increased the T_p and increase in TTP (TTP*PD) decreased the T_p.

6. Conclusion

Numerical model for the heat transfer during friction stir welding of AA6061-T6was generated. The temperature profile was found to be asymmetric and the T_p reached was between 85-90% of the liquidus temperature of the material welded. The temperature profile was dependent more on SD and TTS and TRS. The variation of PD has very insignificant role in obtaining the T_p. Specifically increase in SD increased the T_p during FSW.

References

[1] He X, Gu F, Ball A. A review of numerical analysis of friction stir welding. *Progress in Materials Science*. 2014 8;**65**:1-66.

[2] Sharma HK, Bhatt K, Shah K, Joshi U. Experimental Analysis of Friction Stir Welding of Dissimilar Alloys AA6061 and Mg AZ31 Using Circular Butt Joint Geometry. *Procedia Technology*. 2016 ;**23**:566-72.

[3] Tufaro LN, Manzoni I, Svoboda HG. Effect of Heat Input on AA5052 Friction Stir Welds Characteristics. *Procedia Materials Science*. 2015 ;**8**:914-23.

[4] Buffa G, Campanella D, Pellegrino S, Fratini L. Weld quality prediction in linear friction welding of AA6082-T6 through an integrated numerical tool. *Journal of Materials Processing Technology*. 2016 5;**231**:389-96.

[5] Buglioni L, Tufaro LN, Svoboda HG. Thermal Cycles and Residual Stresses in FSW of Aluminum Alloys: Experimental Measurements and Numerical Models. *Procedia Materials Science*. 2015;**9**:87-96.

[6] Chen CM, Kovacevic R. Finite element modeling of friction stir welding—thermal and thermomechanical analysis. *International Journal of Machine Tools and Manufacture*. 2003;**43**(13):1319-26.

[7] Elatharasan G, Kumar VSS. An Experimental Analysis and Optimization of Process Parameter on Friction Stir Welding of AA 6061-T6 Aluminum Alloy using RSM. *Procedia Engineering*. 2013;**64**:1227-34.

[8] Comsol. Available from: https://www.comsol.co.in/model/friction-stir-welding-of-an-aluminum-plate-461

[9] Nandan R, DebRoy T, Bhadeshia HKDH. Recent advances in friction-stir welding - Process, weldment structure and properties. *Progress in Materials Science*. 2008;**53**(6):980-1023.

[10] Nandan R, Roy G, Debroy T. Numerical simulation of three-dimensional heat transfer and plastic flow during friction stir welding. *Metallurgical and Materials Transactions A*. 2006;**37**(4):1247-59.

[11] Nandan R, Roy GG, Lienert TJ, DebRoy T. Numerical modelling of 3D plastic flow and heat transfer during friction stir welding of stainless steel. *Science and Technology of Welding & Joining*. 2006;**11**(5):526-37.

[12] Nandan R, Roy GG, Lienert TJ, Debroy T. Three-dimensional heat and material flow during friction stir welding of mild steel. *Acta Materialia*. 2007;**55**(3):883-95.

[13] Ulysse P. Three-dimensional modeling of the friction stir-welding process. *International Journal of Machine Tools and Manufacture*. 2002;**42**(14):1549-57.

[14] Dong P, Lu F, Hong JK, Cao Z. Coupled thermomechanical analysis of friction stir welding process using simplified models. *Science and Technology of Welding & Joining*. 2001;**6**(5):281-7.

[15] Heurtier P, Jones MJ, Desrayaud C, Driver JH, Montheillet F, Allehaux D. Mechanical and thermal modelling of Friction Stir Welding. *Journal of Materials Processing Technology*. 2006;**171**(3):348-57.

[16] Ian Mitchell. Residual stress Reduction During Quenching of Wrought 7075 Aluminum alloy [MS Thesis]: Worcester Polytechnic Institute; 2004.

[17] Colegrove PA, Shercliff HR. 3-dimensional Flow and Thermal Modelling of the Friction Stir Welding Process. Proceedings of the 2nd International Symposium on Friction Stir Welding; 2000.

[18] Hwang Y-M, Kang Z-W, Chiou Y-C, Hsu H-H. Experimental study on temperature distributions within the workpiece during friction stir welding of aluminum alloys. *International Journal of Machine Tools & Manufacture*. 2008;**48**:778-87.

[19] Padmanaban R, Kishore VR, Balusamy V. Numerical Simulation of Temperature Distribution and Material Flow During Friction Stir Welding of Dissimilar Aluminum Alloys. *Procedia Engineering*. 2014 ;**97**:854-63.